BJES Basrah Journal for Engineering Sciences

Basrah Journal for Engineering Sciences, Vol. 25, No. 2, (2025), 30-37

Original Article

Journal homepage: https://bjes.edu.iq/bjes
ISSN (Online): 23118385, ISSN (Print): 18146120

Determination of the Stress Intensity Factor in a Sandwich Structure with a Hexagonal Core under Various Loading Conditions

Esraa Sabih Talib [1]*, Rafil Mahmood lafta [2]

[1,2] *Department of Mechanical Engineering, College of Engineering, University of Basrah, Basrah, Iraq*
E-mail addresses: pgs.asraa.sabih@uobasrah.edu.iq , rafil.laftah@uobasrah.edu.iq

Article Info

Article history:
Received: 3 April 2025
Revised: 12 June 2025
Accepted: 21 June 2025
Published: 31 December 2025

Keywords:
Sandwich structure, Hexagonal core, XFEM, Stress intensity factor, Equivalent modulus of elasticity.

https://doi.org/10.33971/bjes.25.2.4

Abstract

Due to the significance of structural sandwiches with hexagonal cores, utilized in various applications including aerospace, marine industries, and rail transport, and their design that imparts superior strength compared to conventional forms. In this paper, fracture behavior of these structural sandwiches was examined. Initially, the equivalent modulus of elasticity was empirically determined for many cell side lengths, utilizing the stress-strain relationship derived from tensile tests on hexagonal specimens. The fracture behavior was analyzed numerically using Abaqus software. The core and the complete sandwich structure were examined under various loads, including tensile and shear forces. The influence of the hexagonal cell dimensions on the fracture modules and the stress intensity factor (SIF), was assessed. It was observed that when the cell thickness remains constant while the side length varies, the SIF increases with the increasing in side length. This leads to the influence of stiffness, where it decreases with the increase in side length of the cell core. For instance, when the side length is 10, the stress intensity factor is 4.821, while when the side length is 20, the stress intensity factor becomes 22.35. A relationship was found between the stress intensity factor and thickness, similar to the tension case. However, here, a relationship between (kI) and the (a/tc) ratio was established.

1. Introduction

The sandwich structure is a unique configuration of composite materials formed by applying two rigid, thin shells to an extremely lightweight, thick core, as shown in Fig. 1. The fundamental material generally has moderate strength; yet its increased thickness imparts significant bending stiffness to the sandwich composite while maintaining a low overall density [1]. The characteristics of the face, core materials, and geometry affect the mechanical performance of a sandwich structure [2]. In the sandwich structure, the core layer is situated at the center. Its main role is to increase the thickness of the sandwich without adding much weight while also providing compressive and shear strength to the structure [3-5].

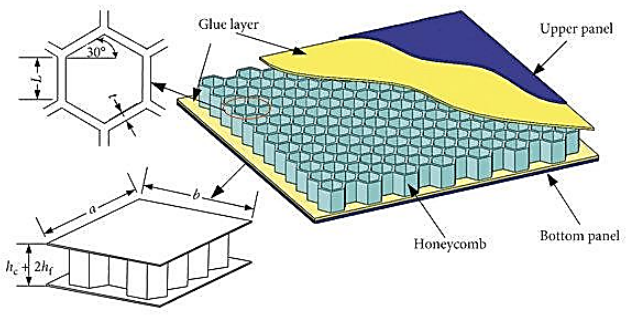

Fig. 1 Sandwich Structure with hexagonal core [6].

Cores can be classified into classical and creative types. The classical cores include honeycomb, foam, corrugated, and truss cores.

Creative cores encompass derived, hollow, pyramidal, graded, hybrid, folded, smart, and folded cores [7].

Sandwich structures are used in various applications, especially in the aviation and marine industries. These structures often utilize honeycomb core materials. Key points include that in 1992, Bitzer from Hexcel provided an overview of honeycomb core materials and their applications. Sandwich structures with honeycomb cores are used in every twin-engine aircraft or more in the Western world. Boeing aircraft, such as the Boeing 757/767 and the Boeing 747, feature a significant portion of wet surfaces made of honeycomb sandwich structures. In aerospace and aircraft, planes like the Beech Starship and spacecraft structures rely on honeycomb sandwich structures made from graphite and Kevlar. In marine applications, the U.S. military uses honeycomb sandwich structures to reduce weight above the waterline in ships and vessels. The Royal Swedish Navy and the Royal Australian Navy also use sandwich structures made of fiberglass and graphite [8].

The first documented application of the sandwich composite materials occurred during the Second World War on the Mosquito and Vampire aircraft, where end-grain balsa was used as the core material, and plywood was used for the skin [9].

Faidallah et al. in 2023 executed the manufacture and characterization of 3D-printed two different types of sandwich structures, “honeycomb and rhombus.” observed that due to their reliable core structure, the rhombus sandwich samples demonstrated the best tensile strength, reaching 23.01 MPa, which was 15.3% higher than the honeycomb [10].

Qi et al. in 2022 studied the buckling load conditions of the composite sandwich structure (CSS) reinforced with a layer of honeycomb filled with viscoelastic damping material. found that the buckling load significantly increases with the width of the composite structure, while it decreases with an increase in the length of the sandwich structure [11].

In 2015, Chauhan et al. [12] and Mashjel et al. [13] demonstrated an innovative approach to calculating the stress intensity factor for a plate with circular holes subjected to a loading. The approach depended on deriving the complex stress function in series form through a complex variable approach by summation method combined with it. Showed that the value of SIF is affected by several parameters, including plate dimensions, material features, hole geometry, and loading type.

In 2024, three equivalent modeling methodologies were used for a dynamic model of honeycomb structures: one of these methods depended on server panel theory, another method depended on Hoff's theory, and Gibson's method. It was found that the three methods used were correct, and the best method was the classical Gibson method, which had a lower error rate than the other; that method was studied by Yasin et al. [14].

In 2021, Farrokhabadi et al. examined the response of sandwich panels under bending conditions. This sandwich is filled and unfilled with sine and square corrugated cores. They applied the sample properties to the ABAQUS software for finite element solution-based three-point bending testing and numerical analysis. They observed that polyurethane foam increases energy absorption and the structure's longevity. For sine and square corrugated cores, the foam-filled samples absorbed 2.5 times more energy than the foam-free ones [15].

Wang et al. in 2019 tested three large-sized specimens of sandwiches consisting of laminate skins from plain weave carbon fabric and of aramid core. A linear response of displacement and strain appears with the increased load. Through a combination of theoretical analysis and the finite element method, the various loads, shear field, and overall buckling load were predicted [16]. SIF is calculated using the concepts of the extended finite element method (XFEM) in ABAQUS.

XFEM is used to determine the SIF in core plate of sandwich with different shapes and sizes cells and load type. This system needs to find the SIF at the crack tip. Through (XFEM), XFEM is used to determine the SIF in the core plate of a sandwich with different shapes and sizes of cells and load types. These needs finding the SIF at the crack tip through XFEM, to the finite element approximation, discontinuous enrichment functions are added to address the presence of the crack. When the FEM is varied, there is no need to reconstruct the crack domain, and the discontinuity is mesh independent [18].

This study attempts to reduce the complexity of the hexagonal configuration of the sandwich structure core by simulating an equivalent plate with the same elastic modulus as the sandwich. This approach facilitates the calculation of the fracture factor of the hexagonal shape using the equivalent plate, which is determined both practically and theoretically.

2. The Extended Finite Element Method (XFEM)

XFEM is a numerical method that extends the classical FEM approach by expanding the solution space to encompass differential solutions of discontinuous function equations. This method was developed to address problems with specific features that cannot be efficiently solved by mesh refinement. One of the initial applications was modeling fractures in materials. This original development incorporates a basis that includes the displacement of the fracture opening, augmenting the normal polynomial basis functions with discontinuous basis functions that represent the interaction between nodes and elements intersected by the fracture. A notable feature of XFEM is that it does not require updating the finite element mesh to track the fracture path in such problems. This method is generally used to address problems related to material interfaces, regular meshes of fine structural features such as voids, singularities, and other problems where a local feature can be described by basic functions [18].

XFEM was developed by Feng et al. [19] to address problems of discontinuous fractures in the displacement field of finite elements, which stemmed from the generalized finite element approach proposed by Melenk et al. [20, 21]. Before the advent of XFEM, fracture propagation was primarily approximated using remeshing techniques and incorporating cohesive elements [22, 23]. XFEM has been used with enrichment functions to simulate crack problems, including displacement discontinuities and singularities, as in the equation (1).

$$u^h(x) = u^{FE} + u^{enr} = \sum_{j=1}^{n} N_j(x)u_j + \sum_{h}^{m} N_k(x)\,\psi(x)\,a_k \qquad (1)$$

Where $N_j(x)$ denotes the usual nodal shape functions, u_j is the vector of uniform degrees of nodal freedom in the FEM, a_k is the additional set of freedom degrees to the conventional FE model, and $\psi(x)$ is the discontinuous enrichment function [18].

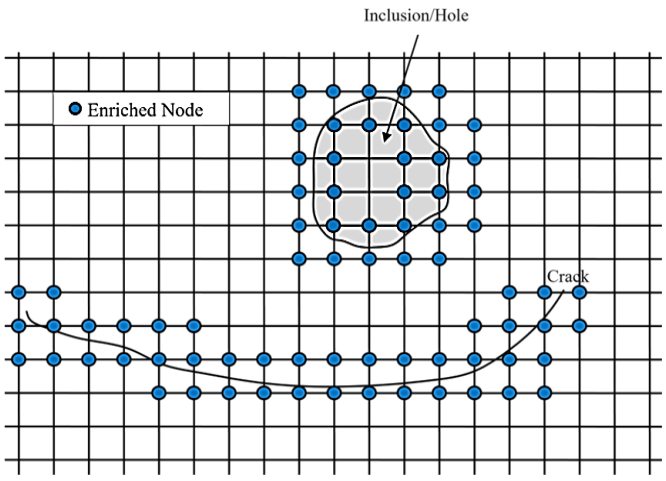

Fig. 2 The enrichment domain simplification [18].

3. Stress intensity factor

Stress Intensity Factor (SIF) has been utilized in fracture mechanics to determine stress concentration at the crack tip, especially due to the application of residual stresses. SIF is

critical in brittle materials for defining failure criteria. Homogeneous Linear Elastic Fracture Mechanics (LEFM) materials contain the SIF, which typically represents the same magnitude. SIF can be determined through its definition, which relates it to the stress field, necessitating accurate computation of stress components, from which SIF is derived by extrapolation to the crack tip. Given that stresses are analyzed at integration points and the crack tip position at the element node, this calculation does not fully align with the definition of the (K_I) [24].

In finite element analysis, the critical parameters to evaluate the (SIF) values in linear elastic fracture mechanics are the stress field and displacement in proximity to the crack tip. These parameters are even used to predict catastrophic propagation of cracks under special loading conditions. There are different methods for calculating K_I values, e.g., the "virtual slit extension method" and integer J and displacement correlation methodologies. SIF can be divided into two classifications: direct approach and energy approach. The direct method associates the SIF with the FE return technique, whereas the alternative method depends on the arithmetic value of the energy release rate (G) [25].

The stress intensity factor of mode I can be calculated by the general equation:

$$K_I = Y\sigma\sqrt{\pi a} \quad (2)$$

Where Y is the geometric factor dependent on load and geometry, σ the normal tension, a is the length of the crack [24].

4. Properties and dimensions of the hexagonal core

This study utilized sandwich core plates composed of carbon steel, characterized by a modulus of elasticity (Es) of 189 GPa and a Poisson's ratio of 0.3. It comprises a hexagonal core of sandwich structure with varying cell dimensions as shown in Fig. 3.

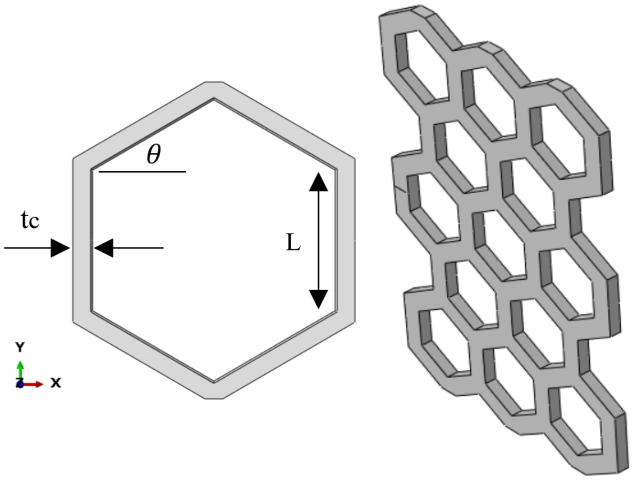

Fig. 3 Dimensions of the hexagonal shape.

5. Equivalent of hexagonal core

Studying the properties of the equivalent hexagonal shape helps reduce the time required for modeling and numerical analysis. The hexagonal shape is complex in terms of mesh arrangement, which requires more time and effort. It is necessary to reduce complexity by developing an equivalent shape for the hexagon, both practically and theoretically. A model of a hexagonal core was created using FEA to calculate the elastic modulus for the x and y directions (Ex = Ey = Ez = Eeq). Also, calculated equivalent volume of hexagonal (Veq).

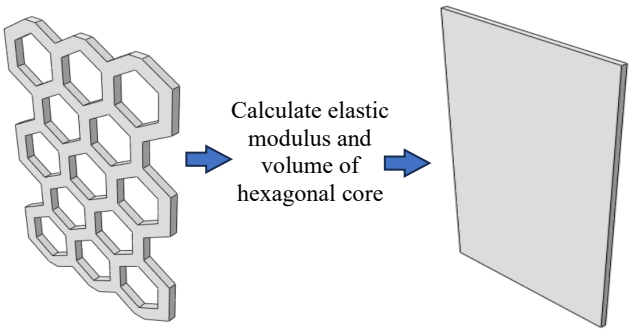

Fig. 4 hexagonal core with equivalent plate.

5.1. Experimental procedure

The equivalent modulus of elasticity for the hexagonal core of the sandwich structure was experimentally calculated by applying tensile loading on the samples in the tension direction. Subsequently, from the stress-strain curve, the equivalent modulus of elasticity was calculated for multiple samples with different side lengths (10, 20, 30, 40), as shown in Fig. 5. After calculated the experimental elastic modulus (Eex) as in Table 1, it was crated relation of Eex/Es with ratio of a/L as in Fig. 6.

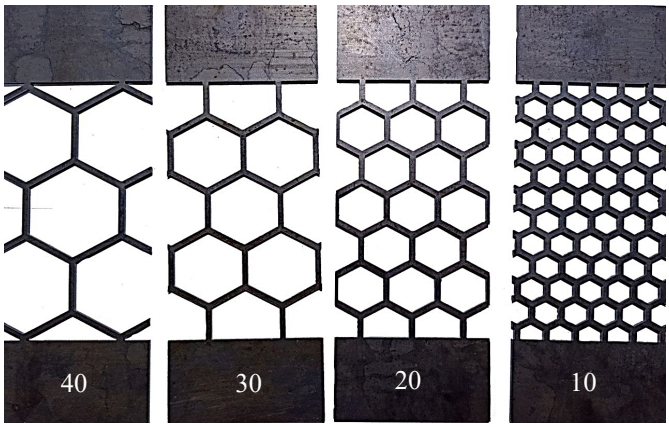

(a)

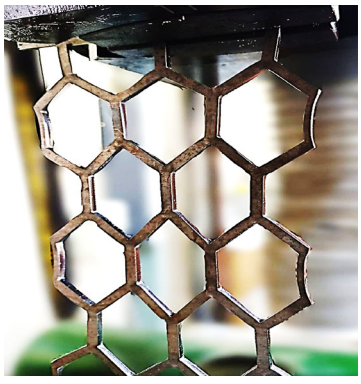

(b)

Fig. 5 Sample of hexagonal core, **(a)** samples with different side length, **(b)** sample during test.

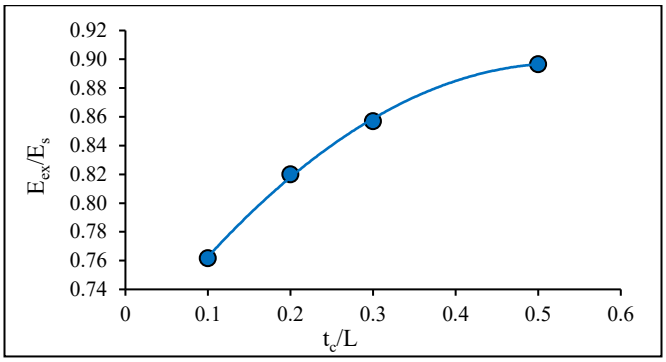

Fig. 6 Relationship between equivalent young modulus to young modulus of solid ratio and tc/L.

Table 1 presents the results of the experiments, indicating that the elasticity modulus of the steel, Es, is 189 GPa, determined by the tensile test performed on the sample prior to its transformation into a hexagonal configuration. The Eeq denotes the computed equivalent modulus of elasticity.

Table 1. experimental result of elastic modulus.

Es = 189 Gpa		
L (mm)	tc/L	Eex (GPa)
40	0.1	144
30	0.2	155
20	0.3	162
10	0.5	169.5

Equation (3) presents the important relation shape that helps us to determine the equivalent elasticity modulus of hexagonal from solid elastic modulus:

$$E_{eq} = [-0.727(t_c/L)^2 + 0.7712(t_c/L) + 0.6929]\, E_s \quad (3)$$

5.2. Theoretical setup of equivalent elastic modulus

The equivalent modulus was calculated theoretically through the ABAQUS program, where the hexagonal core was modeled and the sample was subjected to tension (Fig. 7). The equivalent modulus of elasticity was also found through a stress-strain diagram. The experimental and theoretical results were compared, and the error percentage was less than 10%, as shown in Table 2.

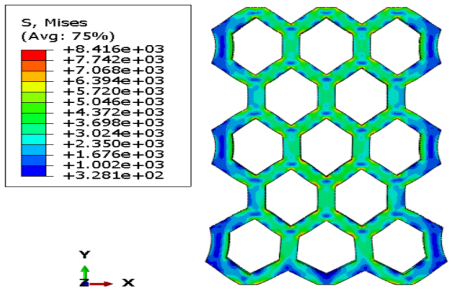

Fig. 7 Hexagonal core under torsion load.

Table 2. data of experimental and theoretical elastic modulus.

Es = 189 GPa				
L	t/L	Eth (GPa)	E_{ex} (Gpa)	Error (%)
40	0.1	130	144	9.7
30	0.2	164	155	6.4
20	0.3	167	162	3.08
10	0.5	171	169.5	0.884

6. Effect of cell Size of hexagonal on the (SIF)

Case 1: Tension load

The stress intensity factor changes with the ratio a/L for each type of hexagonal core structure, with constant tc under tension load as in Fig. 8. It can be observed that hexagonal with 30 has the highest stress intensity factor, followed by hexagonal 20, and then hexagonal 10. This indicates that the different honeycomb designs respond differently to mechanical stress, meaning hexagonal 30 is the strongest in withstanding higher stresses, followed by hexagonal 20 and hexagonal 10. the stress distribution at each specified length as illustrates in Fig. 9, it denoted that the stress increase with increase L this because decrease stiffness of core.

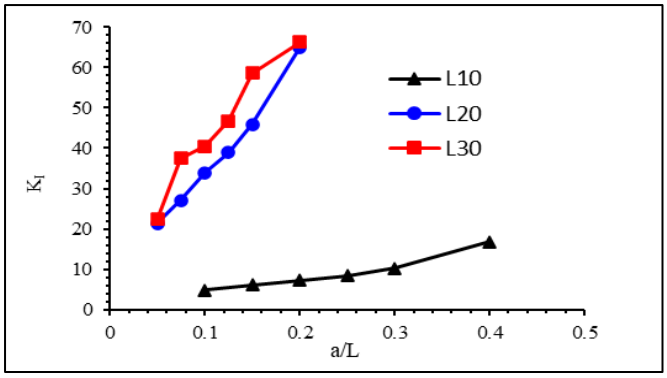

Fig. 8 Effect of crack length to side length ratio on the SIF for hexagonal core with different side length.

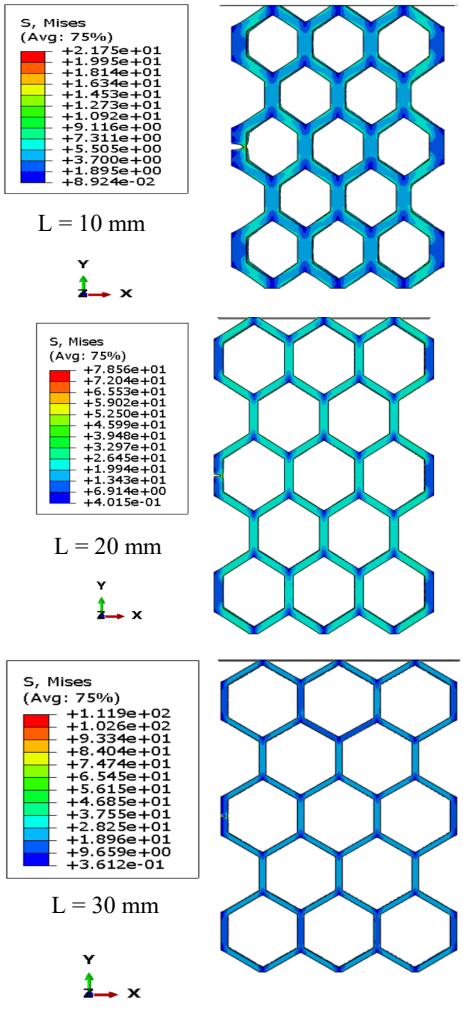

Fig. 9 Stress distribution in hexagonal core with different crack length.

When the side length and crack length were kept constant for more than the cell thickness. It was found that as the thickness of cells increases, the SIF decreases for the same side length, as shown in Fig. 10. Figure 10 illustrates the investigation of stress distribution. This indicated that the length of the side and thickness of the cell influence stiffness, whereas an increase in crack length leads to a decrease in stiffness at variance to increases in cell thickness, leading to an increase in stiffness.

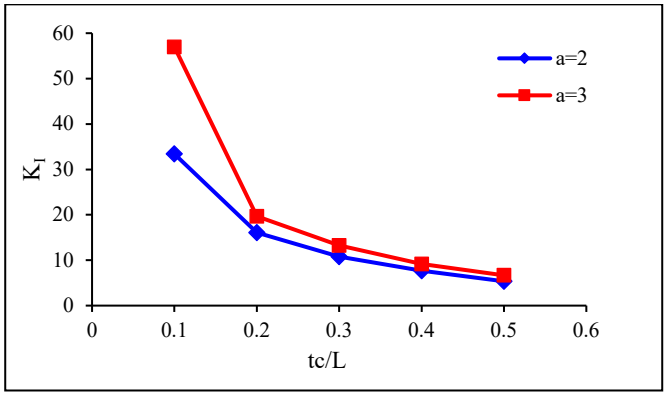

Fig. 10 Reduction of SIF with increasing ratio of thickness to length in crack lengths 2 mm and 3 mm.

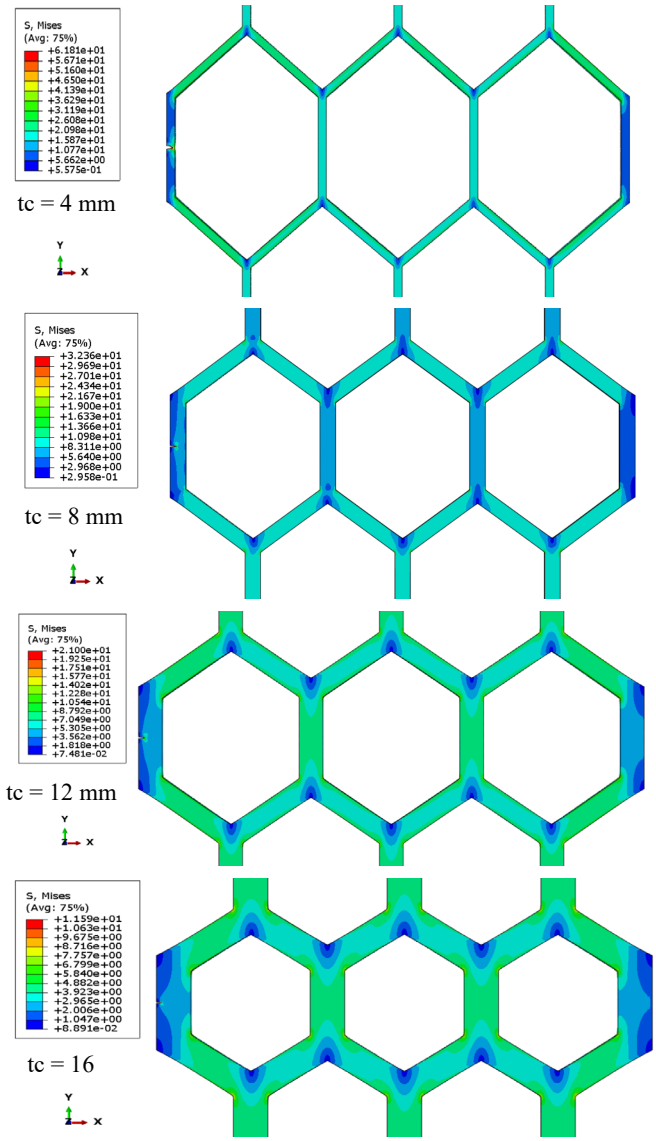

Fig. 11 Stress distribution in hexagonal core with different cell thickness.

6.1. Equivalent hexagonal core tension load

After calculating the equivalent elasticity modulus (Eeq) for the hexagonal structure and considering the variation in the ratio of the length and thickness of the hexagonal cell, it has become easier to calculate the fracture parameters for the hexagonal structure, eliminating the necessity for a complex drawing, which consumes time and effort. As a result, we have derived equations that enable us to calculate K_I of the hexagonal structure using its equivalent. Tables 3, 4, and 5 illustrate the results.

Table 3. data of equivalent stress intensity factor for L = 10 mm.

Side length(L)	Cell thick (t)	Equivalent volume (Veq)
10 mm	5 mm	9500 mm^3

Crack length (a)	K_I	K_{Ieq}	K_I/K_{Ieq}	a/L
1	4.821	16.119	0.29907	0.10
1.5	6.097	21.8203	0.27941	0.15
2	7.33	24.2591	0.30215	0.20
2.5	8.338	27.1412	0.30720	0.25
3	10.214	29.3755	0.34770	0.30
4	16.87	33.0416	0.5105	0.40

Table 4. data of equivalent stress intensity factor for L = 20 mm.

Side length(L)	Cell thick (t)	Equivalent volume (Veq)
20 mm	5 mm	18900 mm^3

Crack length (a)	K_I	K_{Ieq}	K_I/K_{Ieq}	a/L
1	21.39	16.109	1.3277	0.050
1.5	27.086	21.4985	1.25990	0.075
2	33.98	24.2399	1.40181	0.100
2.5	38.897	27.1167	1.43442	0.125
3	45.97	29.3460	1.56647	0.150
4	64.97	33.5012	1.93932	0.200

Table 5. data of equivalent stress intensity factor for L = 30 mm.

Side length(L)	Cell thick (t)	Equivalent volume (Veq)
30 mm	5 mm	25000 mm^3

Crack length (a)	K_I	K_{Ieq}	K_I/K_{Ieq}	a/L
1	22.34	16.2087	1.37826	0.033
1.5	37.442	21.1575	1.7696	0.0500
2	40.53	24.2053	1.67442	0.0667
2.5	46.82	26.3455	1.77714	0.0833
3	58.6	28.5534	2.05229	0.1000

Subsequently, equations were formulated for calculating the SIF for the hexagonal core by establishing its equivalent for various ratios of crack length to side length:

$$K_I = [4.142\ (a/L)^2 - 1.3825(a/L) + 0.3978]\ K_{Ieq} \quad (4)$$

$$K_I = [32.245\ (a/L)^2 - 3.8508\ (a/L) + 1.4203]K_{Ieq} \quad (5)$$

$$K_I = [-64.3\ (a/L)^2 + 16.347\ (a/L) + 0.9549]K_{Ieq} \quad (6)$$

Case 2: Shear load

In case of shear, the hexagonal core is subjected to a load parallel to the *x*-direction and supports the bottom surface. Three hexagonal cores with different side lengths are studied. The a/L extends from 0 to 0.6. At L = 10, the crack length to side length ratio (a/L) leads to a steady rise in the (K_{II}), as shown in Fig. 12. This type of structure demonstrates a gradual tolerance to mechanical stresses. In the case of hexagonal 20, there is an initial rapid increase in K_{II}, which then stabilizes as the ratio (a/L) is increased. The data demonstrates that this type of structure has a high capacity to withstand mechanical stress at the initial stage, and then it stabilizes after reaching a certain point. This property makes it suitable for applications requiring high initial stress tolerance with stable performance over duration. Finally, at L = 30, there is an initial rapid increase in the K_{II}, followed by a slight decrease as the ratio (a/L) increases.

This signifies that this type of structure has the highest strength initially but may slightly decrease in performance over time. This makes it ideal for the applications that require immediate and high stress tolerance, with consideration for structural reinforcement over time. Figure 13 represents the stress around the crack tip, providing flexibility in selecting the suitable design for various applications based on requirements involving stress tolerance.

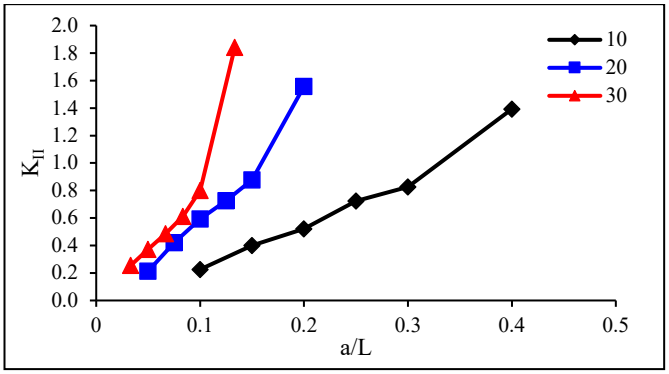

Fig. 12 Effect ratio of crack length to side length in shear load.

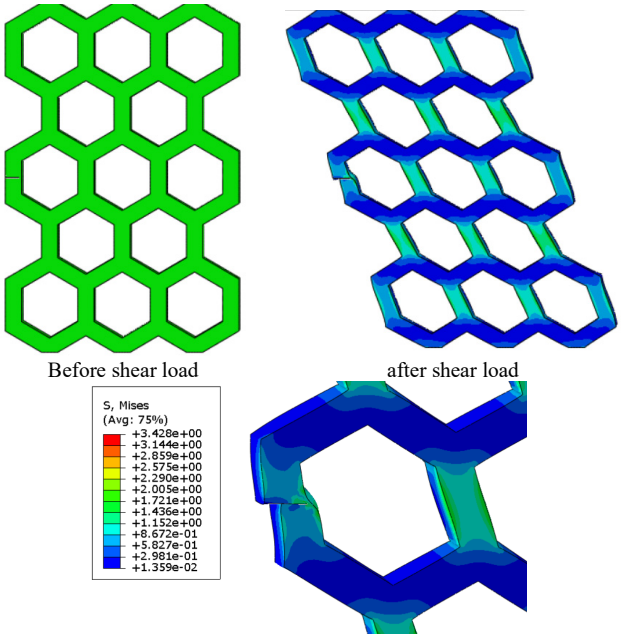

Fig. 13 Stress distribution in cracked hexagonal with shear load.

In the second case of shear load, we studied the effect of changing cell thickness (tc) on SIF. The thickness of the cell gradually increased from 4 mm to 20 mm, with steps of 4 mm. The chart illustrates the relationship between the SIF and the ratio of crack length to cell thickness. The result showed a direct relation between two variables, K_{II} and tc, where the stiffness increases with the increase in thickness of the cell, as represented in Fig.14.

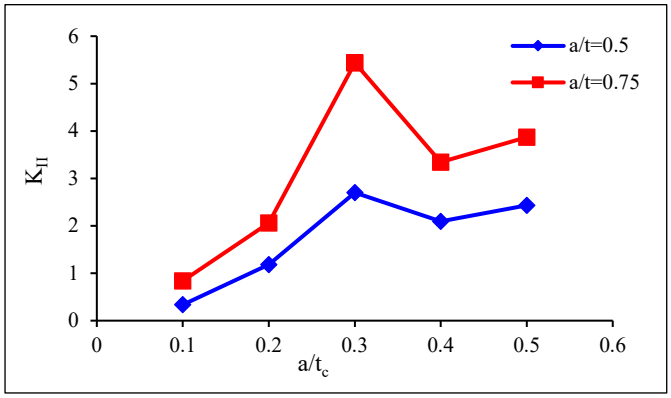

Fig. 14 Effect of crack length to thickness ratio under shear load.

6.2. Equivalent of hexagonal core shear load

An equivalent model for the hexagonal core under shear loading was established by employing the equivalent modulus of elasticity for each side length, analogous to the case of tensile loading. The results obtained provide a correlation that enables the examination of the hexagonal core with its equivalent model, as illustrated in Fig. 15.

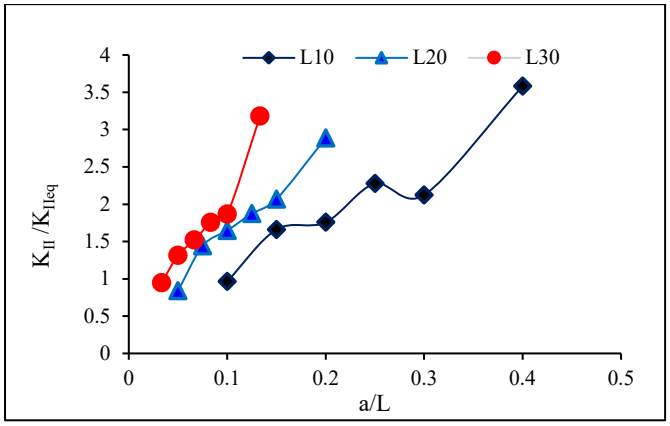

Fig. 15 relation of ratio of stress intensity factor to equivalent with ratio of crack length to side length.

$$K_{II} = [9.4482(a/L)^2 + 3.0015(a/L) + 0.7541]\, K_{IIeq} \quad (7)$$

$$K_{II} = [-0.3752(a/L)^2 + 12.545(a/L) + 0.3348]\, K_{IIeq} \quad (8)$$

$$K_{II} = [147.43(a/L)^2 - 4.1253(a/L) + 1.0333]\, K_{IIeq} \quad (9)$$

7. Sandwich structure

To study crack behavior in sandwich structures, analyzed several crack locations and examined the impact of varying hexagonal core side lengths was examined, as shown in Fig. 16. The results indicate that each crack location has a specific value, which changes with variations in the side length of the hexagonal core, as represented in Figs. 17 and 18.

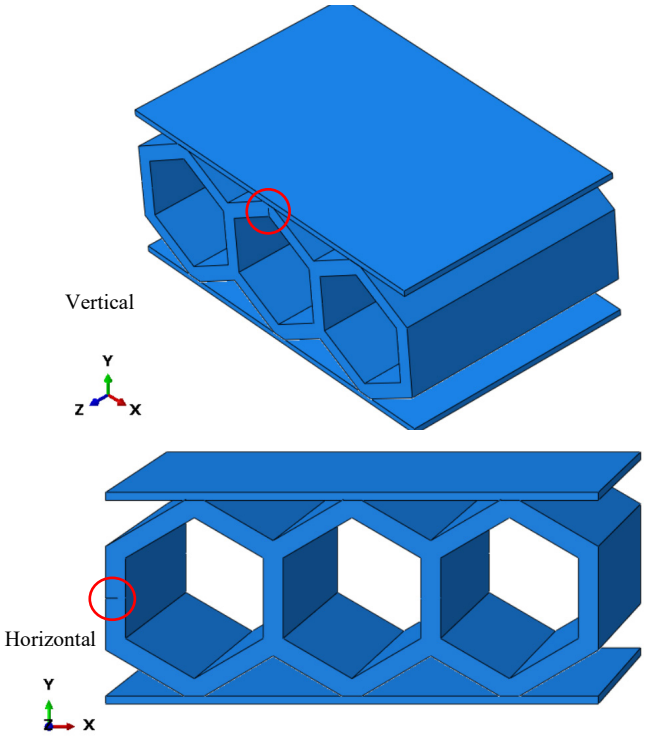

Fig. 16 Sandwich structure with different crack position.

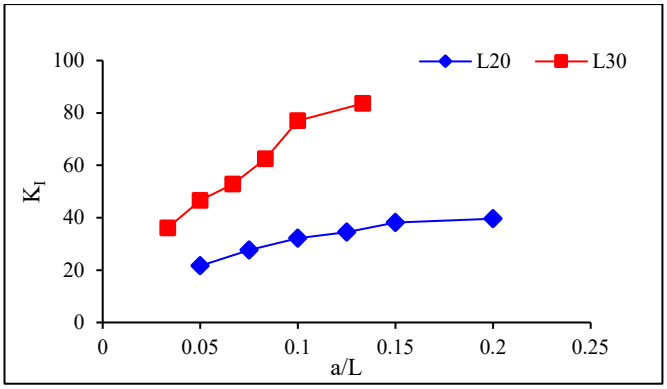

Fig. 17 Effect of a/L on SIF in different horizontal crack position and side length.

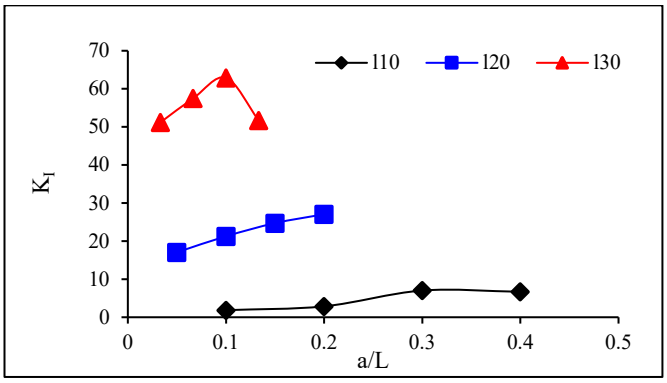

Fig. 18 Effect of a/L on SIF in different vertical crack position and side length.

8. Conclusions

1. In the case of the hexagonal core subjected to tension, two points need to be clarified. The first is that, when the cell thickness has remained constant while the side length varies, the SIF increases with the increase in side length this because decrease stiffness. For instance, when the side length is 10, the stress intensity factor is 4.821, while when the side length is 20, the SIF becomes 22.35 MPa$\sqrt{mm}$ with the cell thickness and crack length remaining constant in both cases.
2. In the second tension case, when the L is constant and the cell thickness varies, there is an inverse relationship between increasing thickness and the stress intensity factor. For example, at thicknesses of 4, 8, 12, 16, and 20 mm, the corresponding K_I values were 33.34, 19.66, 13.29, 13.29, 9.132, and 6.667 MPa$\sqrt{mm}$ respectively.
3. It was observed that when applying shear load to these hexagons, the SIF was lower compared to the tension condition for the same sample, crack length, and thickness. Additionally, in this scenario, a relationship was found between the stress intensity factor and thickness, similar to the tension case. However, here, a relationship between K_{II} and the a/tc ratio was established. The results indicated that as this ratio increases, the stress intensity factor also increases. This demonstrates how different honeycomb sandwich designs respond to mechanical stresses, providing flexibility in selecting the appropriate design for various applications based on stress tolerance requirements.
4. The equivalent modulus of elasticity for the hexagonal core was determined both experimentally and theoretically for different side lengths, with the error margin between the results not exceeding 10%. An equivalent model for the hexagonal core was developed for various side lengths, and a relationship was established to calculate the SIF of the hexagonal core using its equivalent.
5. Regarding the structural sandwich case that includes the core with the skin, two cases of crack position with various lengths of the sides while maintaining constant thickness. The results show that when the crack is horizontal and away from the skin, the SIF is higher. In the horizontal case, the value of the SIF was 24 MPa when the crack length was 3 mm. In the vertical case, which is close to the skin, the stress intensity was 38 MPa.

Symbol	Description
K_I	Stress intensity factor in mode I
K_{II}	Stress intensity factor in mode II
tc	Thickness of cell
L	Side length
E_{th}	Theoretically modulus of elasticity
E_{ex}	Experimental modulus of elasticity
SIF	Stress intensity factor
K_{Ieq}	Equivalent stress intensity factor (mode I)
K_{IIeq}	Equivalent stress intensity factor (mode II

References

[1] V. Birman and G. A. Kardomateas, “Review of current trends in research and applications of sandwich structures,” Composites Part B Engineering, vol. 142, pp. 221-240, 2018. https://doi.org/10.1016/j.compositesb.2018.01.027

[2] L. J. Gibson and M. F. Ashby, Cellular solids: Structure and Properties. Cambridge University Press, 1997.

[3] M. E. Ibrahim, “Nondestructive evaluation of thick-section composites and sandwich structures: A review,” Composites Part A: Applied Science and Manufacturing, vol. 64, pp. 36-48, 2014. https://doi.org/10.1016/j.compositesa.2014.04.010

[4] A. S. Sayyad and Y. M. Ghugal, "Bending, buckling and free vibration of laminated composite and sandwich beams: A critical review of literature," Composite Structures, vol. 171, pp. 486-504, 2017. https://doi.org/10.1016/j.compstruct.2017.03.053

[5] E. Carrera, A. Pagani, and S. Valvano, "Shell elements with through-the-thickness variable kinematics for the analysis of laminated composite and sandwich structures," Composites Part B Engineering, vol. 111, pp. 294-314, 2016. https://doi.org/10.1016/j.compositesb.2016.12.001

[6] W. Wang et al., "Comparative application analysis and test verification on equivalent modeling theories of honeycomb sandwich panels for satellite solar arrays," Advanced Composites Letters, vol. 29, 2020. https://doi.org/10.1177/0963693520963127

[7] X. Wei, D. Li, and J. Xiong, "Fabrication and mechanical behaviors of an all-composite sandwich structure with a hexagon honeycomb core based on the tailor-folding approach," Composites Science and Technology, vol. 184, p. 107878, 2019. https://doi.org/10.1016/j.compscitech.2019.107878

[8] O. T. Thomsen, E. Bozhevolnaya, and A. Lyckegaard, Sandwich Structures 7: Advancing with Sandwich Structures and Materials: Proceedings of the 7th International Conference on Sandwich Structures, Aalborg University, Aalborg, Denmark, 29-31 August 2005. Springer Science & Business Media, 2006.

[9] S. K. Sahu, P. S. R. Sreekanth, and S. V. K. Reddy, "A Brief Review on Advanced Sandwich Structures with Customized Design Core and Composite Face Sheet," Polymers, vol. 14, no. 20, p. 4267, 2022. https://doi.org/10.3390/polym14204267

[10] R. F. Faidallah, M. M. Hanon, Z. Szakál, and I. Oldal, "Study of the Mechanical Characteristics of Sandwich Structures FDM 3D-printed," Acta Polytechnica Hungarica, vol. 20, no. 6, pp. 7-26, 2023. https://doi.org/10.12700/APH.20.6.2023.6.1

[11] D. Qi, Q. Sun, S. Zhang, Y. Wang, and X. Zhou, "Buckling Analysis of a Composite Honeycomb Reinforced Sandwich Embedded with Viscoelastic Damping Material," Applied Sciences, vol. 12, no. 20, p. 10366, 2022. https://doi.org/10.3390/app122010366

[12] M. M. Chauhan, D. S. Sharma, and J. M. Dave, "Stress intensity factor for hypocycloidal hole in finite plate," Theoretical and Applied Fracture Mechanics, vol. 82, pp. 59-68, 2015. https://doi.org/10.1016/j.tafmec.2015.12.005

[13] A. O. Mashjel, R. M. Laftah, and H. I. Khalaf, "Study the effect of perforation type for plate with central crack on the stress intensity factor using the XFEM," Basrah Journal of Engineering Sciences, vol. 21, no. 1, pp. 27-37, 2021. https://doi.org/10.33971/bjes.21.1.5

[14] M. Yasin, K. F. Brethee, and H. M. Hassan, "A study of honeycomb sandwich structure dynamically equivalent modeling methods based on phenotypic analysis and comparison," AIP Conference Proceedings, vol. 3009, p. 030024, 2024. https://doi.org/10.1063/5.0190813

[15] A. Farrokhabadi, S. A. Taghizadeh, H. Madadi, H. Norouzi, and A. Ataei, "Experimental and numerical analysis of novel multi-layer sandwich panels under three point bending load," Composite Structures, vol. 250, p. 112631, 2020. https://doi.org/10.1016/j.compstruct.2020.112631

[16] M.-N. Wang, B. Wang, C. Liu, G. Zhang, Y. Wan, and F. Zhang, "Mechanical Respond and Failure Mode of Large Size Honeycomb Sandwiched Composites under In-Plane Shear Load," Molecules, vol. 24, no. 23, p. 4248, 2019. https://doi.org/10.3390/molecules24234248

[17] M. Eftekhari, A. Baghbanan, and H. Hashemolhosseini, "Determining stress intensity factor for cracked brazilian disc using extended finite element method", International Journal of Scientific Engineering and Technology, Vol. 3, No. 7, pp. 890-893, 2014.

[18] S. Mohammadi, Extended Finite element Method. 2008. https://doi.org/10.1002/9780470697795

[19] Y. Feng, D. Wu, M. G. Stewart, and W. Gao, "Past, current and future trends and challenges in non-deterministic fracture mechanics: A review," Computer Methods in Applied Mechanics and Engineering, vol. 412, p. 116102, 2023. https://doi.org/10.1016/j.cma.2023.116102

[20] J. M. Melenk and I. Babuška, "The partition of unity finite element method: Basic theory and applications," Computer Methods in Applied Mechanics and Engineering, vol. 139, no. 1-4, pp. 289-314, 1996. https://doi.org/10.1016/S0045-7825(96)01087-0

[21] J. M. Melenk, and I. Babuška, "Approximation with harmonic and generalized harmonic polynomials in the partition of unity method," Computer Assisted Methods in Engineering and Science, Vol. 4, Issue 3-4, pp. 607-632, 2023. https://cames.ippt.pan.pl/index.php/cames/article/view/1394

[22] M. S. Shephard, N. A. B. Yehia, G. S. Burd, and T. J. Weidner, "Automatic crack propagation tracking," Computers & Structures, vol. 20, no. 1-3, pp. 211-223, 1985. https://doi.org/10.1016/0045-7949(85)90070-7

[23] J. J. S. Biswakarma, D. A. Cruz, E. D. Bain, J. M. Dennis, J. W. Andzelm, and S. R. Lustig, "Modeling brittle fractures in epoxy nanocomposites using extended finite element and cohesive zone surface methods," Polymers, vol. 13, no. 19, p. 3387, 2021. https://doi.org/10.3390/polym13193387

[24] T. L. Anderson, Fracture Mechanics: Fundamental and Applications, Taylor & Francis Group, LLC, ISBN 978-1-4987-2813-3, 2017.

[25] S. Nama and R. Laftah, "Investigation of Stress Intensity Factor for Corrugated Plates with Different Profiles Using Extended Finite Element (XFEM)," Basrah Journal of Engineering Sciences, vol. 18, no. 1, pp. 1-9, 2018. https://doi:10.33971/bjes.18.1.1